# Dependency of the Power and Delay Domain Parameters on Antenna Height and Distance in Urban Macro Cell

Annika Böttcher*, Christian Schneider†, Peter Vary*, and Reiner S. Thomä†
*Institute of Communication Systems and Data Processing, RWTH Aachen University (Germany)
boettcher@ind.rwth-aachen.de
†Institute of Information Technology, Ilmenau University of Technology (Germany)
christian.schneider@tu-ilmenau.de

***Abstract*—Large scale parameters (LSP) mainly describe the distribution of the transmitted power over different dimensions of the channel. The required statistic is obtained from MIMO channel measurements with an appropriate post processing procedure. In this contribution, we perform the characterization of large scale parameters within an urban macro cell scenario. We focus on investigating the influence of the base station antenna height and the distance between the mobile terminal and the base station. The parameter analysis is conform to the 3GPP SCM and WINNER channel models. We found that parameters as delay spread, K-factor and cross polarization ratio show significant dependency. Because of their potential impact on the system performance these results should be considered and validated in current and future channel models.**

***Index Terms*—large scale parameter, measurement data, channel sounding, spatial channel modeling**

## I. Introduction

For developing and improving wireless communication systems, especially for multi user and multi antenna applications, channel models which reflect the natural behavior of the mobile radio channel are indispensable. Recent channel model developments are the COST [1] and WINNER [2] models, which belong to the geometry based stochastic channel models. Those models are based on large scale parameters (LSP) like the delay spread (DS), the transmission loss (TL), the shadow fading (SF), the narrowband K-factor, the cross polarization ratio (XPR) as well as the angles of arrival and departure. Since these parameters and their corresponding distribution functions play a fundamental role as global scenario dependent parameters, it is essential to analyze to which they are sensitive. Possible influences could be, e.g., the underlying scenario, the propagation condition and setup, the distance between base station (BS) and mobile terminal (MT) as well as the antenna height at both sides. The two latter aspects are of particular importance, because it seems to be possible to develop first single coherencies. For this several contributions can be found already in the open literature. In [3], [4] and [5] the dependency of the TL and the DS with respect to the antenna height for $5.3\,\mathrm{GHz}$ in an urban, suburban and rural environment, for $5.2\,\mathrm{GHz}$ under urban conditions and accordingly for $905 - 915\,\mathrm{MHz}$ in a suburban scenario, measurements has been analyzed. However, the results are not consistent. While in [3] and in [5] the TL increases for decreasing antenna height, in [4] the values of the TL are greater for the higher antenna. A similar contradiction is given for the DS. Whereas [3] and [4] present the same results, the outcomes in [5] are the other way round. In [6] the TL regarding the distance in microcells of urban and suburban environments has been analyzed and in [7] as well as in [8] the main focus is placed on the behavior of the K-factor and the XPR versus the distance of fixed wireless channels in a suburban scenario. Although a lot of research is made in this topic, it is remarkable that the results are sometimes inconsistent. Therefore and since the outcomes are not fully up to date, a revision of existing results and new analysis to elucidate this subject is necessary. For this reason in our contribution the dependency of the LSPs of the power and delay domain with regard to different antenna heights and to various distance ranges between the mobile terminal (MT) and the base station (BS) is analyzed and evaluated. The underlying measurement data sets are taken from an extensive MIMO channel sounding campaign in Ilmenau, Germany.

This work has been supported by the UMIC Research Centre, RWTH Aachen University.

## II. MIMO Channel Measurement Campaign

The measurement and antenna setups that match the requirements of the 3GPP Long Term Evolution (LTE and LTE-A) [9] are described in detail in [10]. The channel sounding was performed at $2.53\,\mathrm{GHz}$ in a band of $2 \times 45\,\mathrm{MHz}$. To allow high resolution path parameter estimations, dedicated antenna arrays are used at the transmitter (Tx) and the receiver (Rx). On the Tx side (base station), a uniform linear array is used with 8 dualpolarized (H/V) elements, each of which consists of a stack of 4 patches in order to form a narrow transmit beam in elevation. At the mobile (passenger car), a circular array with 2 rings of 12 patches with H/V polarizations is used. Additionally, a MIMO cube is placed on top. The mobile acts as Rx. For each of the tracks and for each measured snapshot, geo-data information based on GPS, odometer and separated distance measurements via laser is available. A typical length of a track is $50\,\mathrm{m}$ - $70\,\mathrm{m}$. In total the measurement campaign covers 3 base station positions with a height of $25\,\mathrm{m}$ and $15\,\mathrm{m}$ and an additional relay point ($3.5\,\mathrm{m}$) in the middle of the scenario. The intersite distance between the base stations is found to be for BS1-BS2 $= 680\,\mathrm{m}$, BS2-BS3 $= 580\,\mathrm{m}$ and BS3-BS1 $= 640\,\mathrm{m}$. More than 20 individual tracks with more than 120 measurement runs have been performed. For more information about the measurement campaign we refer to [10] and [11].

## III. Data Analysis Procedure

As already mentioned the estimation of the LSPs and the analysis of their behavior with regard to different influences like the antenna height or the distance between MT and BS is very important for current research in the field of mobile radio communication. In the following, the analysis steps of the estimation of the LSPs are introduced.

The RUSK channel sounder provides 4-dimensional channel transfer matrices $H(t, f, s, u)$. The variable $t$ denotes the time instant of a snapshot measurement, $f$ is the frequency and $s$ is the $s$-th Rx and $u$ the $u$-th Tx antenna, respectively. For our evaluation we only use 40 MHz in the lower band. The snapshots where a line of sight (LOS) exists and those where no line of sight (NLOS) is given are separated into two groups and will be analyzed individually. The channel transfer matrices are transformed into channel impulse response (CIR) matrices $h(t, \tau, s, u)$, where $\tau$ denotes delay. Our channel sounder utilizes an automatic gain control (AGC) between the MIMO channels within one snapshot. These AGC values can change along the dimensions $t$, $s$ and $u$ of matrix $h$. Taking this aspect into account the CIRs are sorted into different AGC dependent groups. That means the matrices considered per MIMO subchannel with the same AGC value are grouped together and for each group the following calculations are made separately.

Due to noise that is included in the measured channel data, a noise power estimation and subsequently a thresholding in the delay domain is applied to reduce the effect of the noise. The maximum estimated noise level from all available CIRs per AGC group is selected and is considered as cutting level. Subsequently, a 20 dB quality threshold (QT) is introduced, i.e., only the 20 dB below the maximum peak of the power delay profile (PDP) are considered.

Now the PDP $P(t, \tau)$ is calculated. Therefore, the instantaneous power is estimated, a delay shift removing the shortest base delay is introduced and the dimension of the data by averaging over the (Tx, Rx)-antenna pairs is reduced. This results in the PDP per discrete snapshot $t_0$ denoted by

$$P_{t_0}(\tau) := P(t_0, \tau). \quad (1)$$

For estimating the LSPs, the PDP $P(t, \tau)$ has to be averaged over $N_t(l)$ snapshots, where $N_t$ is variable depending on the size of the stationarity interval. This results in

$$P_{t_l}(\tau) := P(t_l, \tau) = \frac{1}{N_t(l)} \sum_{i=1}^{N_t(l)} P(t_{l_i}, \tau). \quad (2)$$

Here $l$ denotes the number of the stationarity interval which is given by $|t_{l_{N_t}} - t_{l_1}| \leq 10\lambda$, where $\lambda$ is the wavelength corresponding to the carrier frequency of the system. The value of the time $t$ in the middle of the interval is denoted by $t_l$. Based on this preprocessed data the LSP determination is executed. The parameters are estimated for each AGC group and are then averaged except for the K-factor, where the maximum is taken. In this paper only the most important steps of the parameter calculations are presented. A detailed description can be found in [12].

### A. RMS Delay Spread (DS)

The first parameter which is of great interest is the root mean square (RMS) DS. It is determined based on the PDP per stationarity interval and is calculated as follows:

$$\sigma_{t_l} = \sqrt{\left(\sum_{n=1}^{N_\tau} \tau_n^2 p_{t_l}(\tau_n)\right) - \left(\sum_{n=1}^{N_\tau} \tau_n p_{t_l}(\tau_n)\right)^2}, \quad (3)$$

where $p_{t_l}(\tau)$ is the probability density function of $P_{t_l}(\tau)$.

### B. Transmission Loss (TL) and Shadow Fading (SF)

Other important parameters are the TL and the corresponding SF. Based on the total power $P_d$ depending on the distance $d$, the TL is calculated as

$$\text{TL}(d) = 46\text{dBm} - 10\text{dB} - 10\log_{10}(P(d)/0.001) \quad (4)$$

The SF is then given by

$$\text{SF}(d) = \overline{\text{TL}}(d) - \text{TL}(d), \quad (5)$$

where $\overline{\text{TL}}(d) = B + A \cdot \log_{10}(d)$ with appropriate linear regression factors $A$ and $B$. These factors are estimated based on the values of the TL, which were calculated without considering any grouping with respect to the AGC values.

### C. Narrowband K-Factor

For the estimation of the narrowband K-factor the narrowband impulse response is needed. It is calculated as the complex sum over the delay domain of the preprocessed and delay shifted channel impulse response $\tilde{h}(t, \tau, s, u)$ and is given by

$$h_{narr}(t, s, u) = \sum_{i=1}^{N_\tau} \tilde{h}(t, \tau_i, s, u). \quad (6)$$

A detailed description for the estimation of the K-factor for each AGC group is presented in [12]. Using the moment method proposed in [15] the K-factor per stationarity interval and per AGC group results in

$$K(t_l, \text{agc}) = \frac{1}{\frac{\text{E}(\hat{P}_{narr}^{(L)}(t_l, agc))}{m(t_l, \text{agc})} - 1} \quad (7)$$

with

$$m(t_l, \text{agc}) = \sqrt{\text{E}(\hat{P}_{narr}^{(L)}(t_l, agc))^2 - \text{Var}(\hat{P}_{narr}^{(L)}(t_l, agc))} \quad (8)$$

and $\hat{P}_{narr}^{(L)}(t_l, agc)$ is the power of the normalized values of $h_{narr}(t, s, u)$ per stationarity interval and AGC group. To get only one value of the K-factor per stationarity interval the maximum value is chosen

$$K(t_l) = \max_{\text{agc}}(K(t_l, \text{agc})). \quad (9)$$

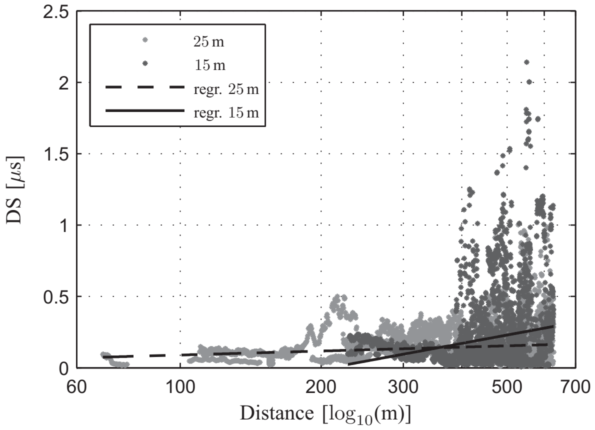


Fig. 1. The delay spread (NLOS) versus the distance for different antenna heights.

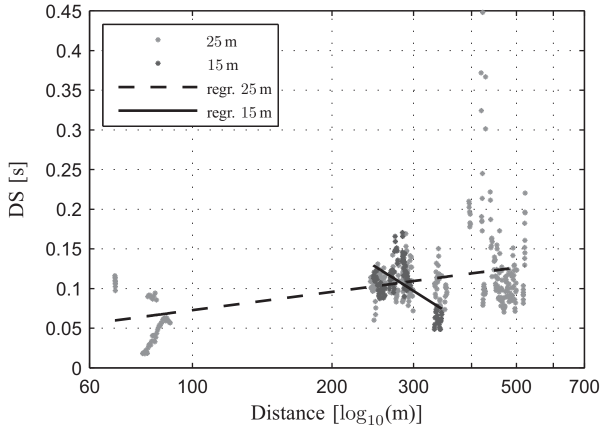


Fig. 3. The delay spread (LOS) versus the distance for different antenna heights.

### *D. Cross Polarization Ratio (XPR)*

It is differentiated between the vertical and horizontal polarization ratio which is denoted by $\mathrm{XPR_v}$ and $\mathrm{XPR_h}$, respectively. The XPR is based on the total power $P_{t_l}$ per stationarity interval. $\mathrm{XPR_v}$ is the ratio of the total power of all vertical-to-vertical channels and vertical-to-horizontal channels, whereas $\mathrm{XPR_h}$ is the ratio of the total power of all horizontal-to-horizontal channels and horizontal-to-vertical channels. The calculation is described as

$$\mathrm{XPR_v}(t_l) = \frac{P_{t_{l\,\mathrm{vv}}}}{P_{t_{l\,\mathrm{vh}}}},\ \mathrm{XPR_h}(t_l) = \frac{P_{t_{l\,\mathrm{hh}}}}{P_{t_{l\,\mathrm{hv}}}} \tag{10}$$

which is in line with [2].

## IV. Empirical Results of Data Analysis

In this section our results for the different LSPs with regard to two different antenna heights and various distance ranges are presented. For the examination all base stations and all tracks are considered at once but distinguished between line of sight (LOS) and non line of sight (NLOS).

### *A. RMS Delay Spread*

Figure 1 shows the DS as a function of the distance and the corresponding linear regression for the two antenna heights (25 m/15 m) in the NLOS case.

One can see that the DS increases with increasing distance in both cases. This is confirmed by Fig. 2 where the cumulative distribution function (CDF) of the DS according to different antenna heights and different distances between MT and BS for NLOS is shown and by Table I where the values for the mean and the standard deviation (std) are summarized. This is due to the fact that with increasing distance the possibility of reflections and diffractions will increase and hence the spreading of the multipath power increases. The same behavior can be observed in the LOS case, which is depicted in Fig 3. The erroneous behavior of the values for the lower antenna height is caused by the lack of data. Therefore no representative (n.r.) assumptions can be made. This holds for the other LSPs in the same manner.

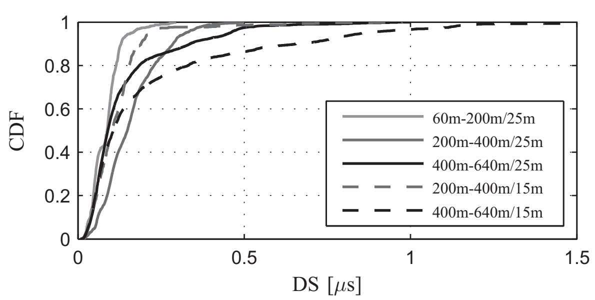


Fig. 2. CDF of the delay spread (NLOS) for different antenna heights and distance ranges.

Worth mentioning is that the values of the DS are more spreaded and they are in average larger for the lower antenna height. This can be explained by the fact that the higher antenna strengthens the strongest multipath or cluster component (in NLOS) and accordingly the direct path (in LOS) relative to the reflected paths. This would cause a higher proportion of the received energy concentrating in the earlier arrivals and resulting in a reduced delay spread. This is conform to the outcomes in [5], while in [6], [4] and [3] the contrary behavior is observed. A possible explanation might be that the two latter publications used a higher center frequency.

### *B. Transmission Loss and Shadow Fading*

The results for the TL for NLOS are presented in Fig. 4 and the corresponding model for the linear regression for a distance $d$ with $60 \leq d \leq 640$ is given by:

$$\overline{TL}_{\mathrm{NLOS}} = \begin{cases} 28.43 + 42.69 \cdot \log_{10}(d), & \mathrm{h_{BS}} = 25\,\mathrm{m}, \\ -69.74 + 82.24 \cdot \log_{10}(d), & \mathrm{h_{BS}} = 15\,\mathrm{m}. \end{cases} \tag{11}$$

| | NLOS | | LOS | |
|---|---|---|---|---|
| | mean | std | mean | std |
| 60m-200m/25m | $0.09\,\mu s$ | $0.04\,\mu s$ | $0.06\,\mu s$ | $0.03\,\mu s$ |
| 200m-400m/25m | $0.16\,\mu s$ | $0.09\,\mu s$ | $0.11\,\mu s$ | $0.03\,\mu s$ |
| 400m-640m/25m | $0.14\,\mu s$ | $0.14\,\mu s$ | $0.12\,\mu s$ | $0.06\,\mu s$ |
| 60m-200m/15m | n.a. | n.a. | n.a. | n.a. |
| 200m-400m/15m | $0.12\,\mu s$ | $0.09\,\mu s$ | n.r. | n.r. |
| 400m-640m/15m | $0.23\,\mu s$ | $0.29\,\mu s$ | n.a. | n.a. |

TABLE I
Values for the mean and std for the delay spread for different antenna heights and distance ranges.

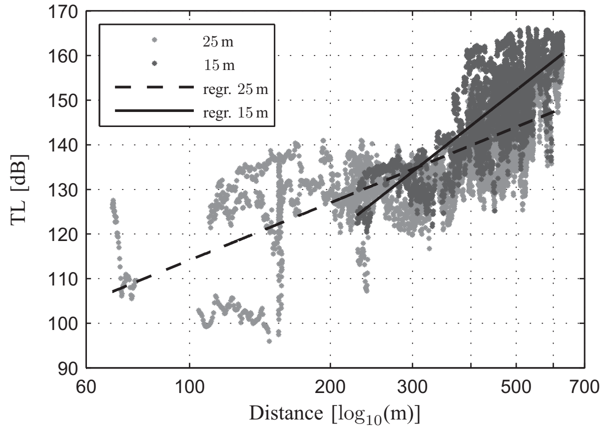


Fig. 4. The transmission loss (NLOS) versus the distance for different antenna heights.

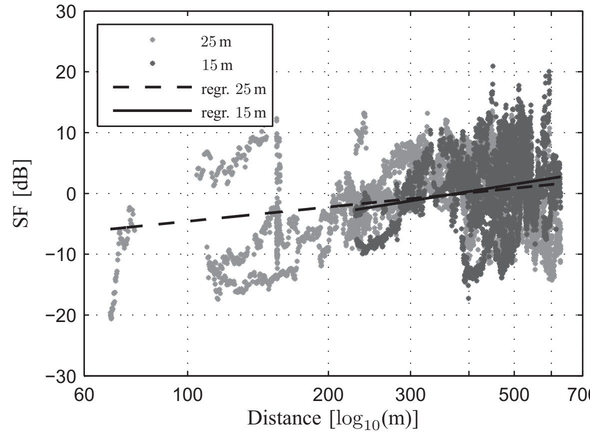


Fig. 5. The shadow fading (NLOS) versus the distance for different antenna heights.

The values increase for increasing distance in both cases which is in line with [6], while the gradient for the lower antenna height is much greater. This is what we expected, because with decreasing antenna height the radio waves suffer on the way between BS and MT from more multipath effects, which cause more power loss and additional delay.

The SF is the difference between TL and the corresponding linear regression and is shown in Fig 5. To be mentioned is that the values decrease for increasing distance in the range of 400 m - 700 m, i.e., the deviation of the values of the TL at the mean decreases in this distance range. The behavior of the values of the TL and the SF in the LOS case is similar and is neglected here.

## C. Narrowband K-factor

Table II presents the estimated values for the mean and the std of the narrowband K-factor with regard to different antenna heights and distance ranges. It is clearly visible that the values of the mean and the std decrease with increasing distance range for both antenna heights in both propagation cases (NLOS and LOS). That is confirmed by the outcomes of [7] and [8]. Additionally the values for the lower antenna height are minimally smaller then for the greater one. As already mentioned for the DS both effects are explained by the lower concentration of the power on the strongest multipath or cluster component (in NLOS) and accordingly the direct path component (in LOS) for higher distance ranges and lower antenna height. This is confirmed by Fig. 6 and Fig. 7, where the K-factor as a function of the distance and accordingly the CDFs are shown for the NLOS case. For the same reason as for the DS in the LOS case no representative assumptions can be made.

| | NLOS | | LOS | |
|---|---|---|---|---|
| | mean | std | mean | std |
| 60m-200m/25m | 7.51 dB | 8.30 dB | 10.40 dB | 6.87 dB |
| 200m-400m/25m | 6.13 dB | 6.74 dB | 10.32 dB | 6.81 dB |
| 400m-640m/25m | 5.24 dB | 6.62 dB | 5.86 dB | 5.22 dB |
| 60m-200m/15m | n.a. | n.a. | n.a. | n.a. |
| 200m-400m/15m | 6.06 dB | 7.47 dB | n.r. | n.r. |
| 400m-640m/15m | 4.35 dB | 6.55 dB | n.a. | n.a. |

TABLE II
VALUES FOR THE MEAN AND STD FOR THE K-FACTOR FOR DIFFERENT ANTENNA HEIGHTS AND DISTANCE RANGES.

## D. Cross Polarization Ratio

Here only the results for the horizontal cross polarization ($XPR_h$) are presented. It should be noted that the vertical cross polarization ($XPR_v$) behaves equivalent with the difference that the values are in general 2 dB - 3 dB greater. Figures 8 and 9 show the scatter plot and accordingly the CDF of the $XPR_h$ with regard to the distance and the antenna height for NLOS.

Table III summarizes the results. The figures and the table clearly show that the values for the XPR decrease significantly with the distance in the NLOS case, which is in line with the results in [7] and [8]. That means if the BS and the MT are more distant the multipath propagation (multiple reflections and diffractions) reduces the XPRs. It is very important to take this aspect into account, because many MIMO systems use different polarizations. Under LOS condition there are only slight reductions in the values. That reflects what we expected and is explained by the existence of a very dominant path or cluster.

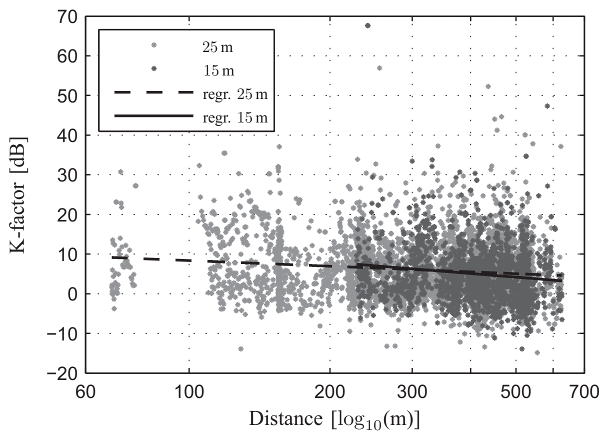


Fig. 6. The K-factor (NLOS) versus the distance for different antenna heights.

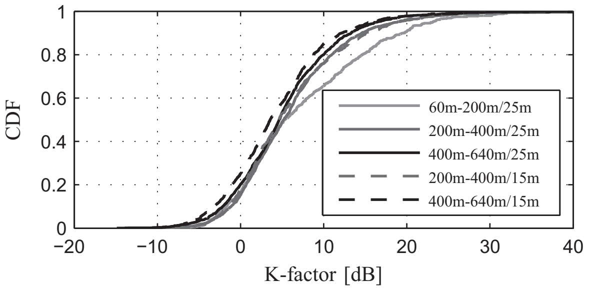


Fig. 7. CDF of the K-factor (NLOS) for different antenna heights and distance ranges.

## V. Conclusion

Essential large scale parameters as the transmission loss (TL), shadow fading (SF), delay spread (DS), narrowband K-factor as well as the cross polarization ratio (XPR) are derived from a MIMO channel measurement campaign with 2 different base station heights and at the frequency of 2.53 GHz. The post processing of the data was in line with the well accepted 3GPP SCM and WINNER channel models. We found out that under NLOS conditions parameters as DS, K-Factor and XPR significantly depend on the considered BS height and on the absolute distance to the MT. While the DS increases with increasing distance, the K-factor and the XPR decrease. Furthermore this effect is emphasized if the BS height is decreased. As a possible consequence a mobile communication system relying on a high cross polarization separation will suffer with higher distance between BS and MT as well as with decreasing BS height. Based on these achievements, deriving new or improved parameter models and rules including the most significant effects of the antenna height of the BS and of the distance variations between MT and BS is part of the current activities in progress and future work plans.

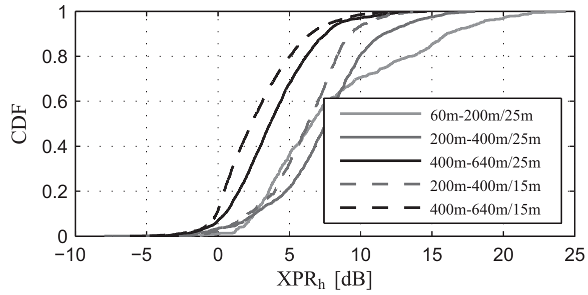


Fig. 9. CDF of the horizontal cross polarization ratio (NLOS) according to the distance for different antenna heights.

| | NLOS | | LOS | |
|---|---|---|---|---|
| | mean | std | mean | std |
| 60m-200m/25m | 8.09 dB | 5.33 dB | 7.63 dB | 4.66 dB |
| 200m-400m/25m | 7.40 dB | 3.62 dB | 11.63 dB | 3.67 dB |
| 400m-640m/25m | 3.87 dB | 2.88 dB | 6.96 dB | 2.52 dB |
| 60m-200m/15m | n.a. | n.a. | n.a. | n.a. |
| 200m-400m/15m | 6.10 dB | 2.83 dB | n.r. | n.r. |
| 400m-640m/15m | 2.79 dB | 2.77 dB | n.a. | n.a. |

TABLE III
Values for the mean and std for the horizontal XPR for different antenna heights and distance ranges.

## References

[1] http://www.cost.esf.org
[2] http://www.ist-winner.org
[3] X. Zhao, J. Kivinen, P. Vainikainen, K. Skog, "Propagation Characteristics for Wideband Outdoor Mobile Communications at 5.3 GHz", *IEEE Journal on Selected Areas in Communications*, Vol.20, Issue 3, 2002.

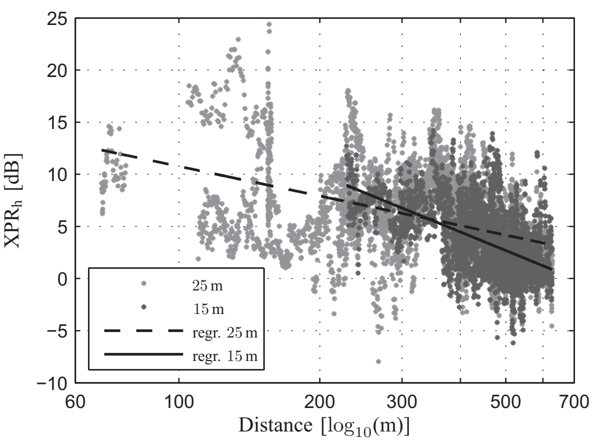


Fig. 8. The horizontal cross polarization ratio (NLOS) versus the distance for different antenna heights.

[4] A. Hong, R. S. Thomä, "Experimental Study on the Impact of the Base Station Height on the Channel Parameters", *Int. IEEE Workshop on Smart Antennas (WSA 2009)*, Berlin, Germany, 2009.
[5] E. Benner, A. B. Sesay, "Effects of Antenna Height, Antenna Gain, and Pattern Downtilting for Cellular Mobile Radio", *IEEE Transactions on Vehicular Technology*, Vol. 45, Issue 2, 1996.
[6] K. L. Blackard, M. J. Feuerstein, T. S. Rappaport, S. Y. Seidel, H. H. Xia, "Path Loss and Delay Spread Models as Functions of Antenna Height for Microcellular System Design", *IEEE Vehicular Technology Conference*, 1992.
[7] D. S. Baum, D. Gore, R. Nabar, S. Panchanathan, K. V. S. Hari, V. Erceg, A. J. Paulraj, "Measurement and Characterization of Broadband MIMO Fixed Wireless Channels at 2.5 GHz", *Int. IEEE Conference on Personal Wireless Communications*, Hyderabad , India, 2000.
[8] P. Soma, D. S. Baum, V. Erceg, R. Krishnamoorthy, A. J. Paulraj, "Analysis and Modeling of Multiple-Input Multiple-Output (MIMO) Radio Channel Based on Outdoor Measurements Conducted at 2.5 GHz for Fixed BWA Applications", *Int. IEEE Conference on Communications (ICC 2002)*, New York, NY , USA, 2002.
[9] 3rd Generation Partnerchip Project (3GPP); Technical Specification Group Radio Access Network, "Evolved Terrestrial Radio Access (E-UTRA) and Evolved Universal Terrestrial Radio Access Network (E-UTRAN); Overall description; Stage 2", *TS 36.300, Version 8.12.0, Rel. 8*, 2010.
[10] C. Schneider, G. Sommerkorn, M. Narandzic, M. Käske, A. Hong, V. Algeier, W. Kotterman, R. Thomä, C. Jandura, "Multi-User MIMO Channel Reference Data for Channel Modelling and System Evaluation from Measurements", *Int. IEEE Workshop on Smart Antennas (WSA 2009)*, Berlin, Germany, 2009.
[11] http://www-emt.tu-ilmenau.de/ReferenceScenario/
[12] A. Boettcher, C. Schneider, M. Narandzic, P. Vary, R.S. Thomae, "Power and Delay Domain Parameters of Channel Measurements at 2.53 GHz in an Urban Macro Cell Szenario", *EuCAP*, Barcelona, Spain, 2010.
[13] http://www.medav.de
[14] A. Böttcher, C. Schneider, M. Narandzic, P. Vary, R.S. Thomä, "Estimation of the Radio Channel Parameters from a Circular Array with Directional Antennas", *VTC2011-sring, Budapest, Hungary, 2011*, submitted for publication.
[15] Greenstein, et. al., "Moment method estimation of the Ricean K-factor", *IEEE Commmunication Letters*, Vol.3, Issue 6, 1999.
[16] P. Soma, D.S. Baum, V. Erceg, R. Krishnamoorthy, A.J. Paulraj, "Analysis and modeling of multiple-input multiple-output (MIMO) radio channel based on outdoor measurements conducted at 2.5 GHz for fixed BWA applications ", *IEEE International Conference on Comm., New York, NY, USA, 2002.*